Modelling and Determining Parameters of a Solar Photovoltaic Cell based on Voltage and Current Measurements

Duy C. Huynh[1,*], Loc D. Ho[1], and Matthew W. Dunnigan[2]

ARTICLE INFO

Article history:
Received: 07 December 2022
Revised: 12 February 2023
Accepted: 27 March 2023

Keywords:
SPV cell models
SPV cell parameters
Parameter estimation
Stochastic fractal search algorithm

ABSTRACT

An appropriate model of a solar photovoltaic (SPV) cell is essential for control, operation, and prediction of SPV systems. Simultaneously, it is equally vital for determining as accurately as possible the parameters of that model. There are currently single-diode (SD), double-diode (DD) and triple-diode (TD) SPV cell models needing to be determined for various applications. A simple and effective approach is proposed for determining the parameters of SPV cell models through voltage and current measurements; as well as the transformation of the estimation problem into the optimization problem. Then, stochastic fractal search (SFS) algorithms with the benefits of finding the global optimal solution in a few generations and avoiding getting stuck in locally optimal solutions are proposed to apply for the above one. The achievements are compared to those by other existing algorithms such as a particle swarm optimization (PSO) and Chaos PSO algorithms to validate the proposals.

1. INTRODUCTION

Amongst renewable energy sources, solar energy has been confirmed for its efficiency and popularity in utilization, especially through SPV systems. It is realized that these systems can be easily installed, conveniently maintained, and certainly reduced pollution. These are the reasons why a significant amount of research is devoted in scenarios of irradiation and temperature [1]. Currently, most designs are based on SPV cell models through parameters describing the working process. Each SPV cell model with its parameters will be meaningful to a specific problem. Amongst the models, the SD model is used commonly with an acceptable accuracy [2]. However, the saturation current of the SPV cell is a linear superposition of charge diffusion and recombination. Thus, it is contributed by two Shockley terms or two diodes. Then, the DD model is introduced [3]. Several previous studies show that the DD model obtains greater precision [4]-[5]. Nevertheless, the greater simplicity of the SD model is also an option that should be considered in the research. Meanwhile, the TD model leads to higher precision in describing the losses of the SPV cell. Then, parameter estimation in the above models is necessary and this becomes a challenge. The more precisely the parameters of the models are estimated, the more efficiently the SPV systems can be analyzed, controlled, and operated. There have been several estimation approaches as follows.

The analytical approach utilizes the Lambert W function [6], nonlinear least-squares fitting algorithms [7], and Nyquist and Bode plots-based algorithms [8]. It is considered the simplest approach amongst estimation approaches and is appropriate for the SD model. To the DD and TD models, there is no exact solution for the parameter estimation results because of the high non-linearity of these models [9]-[10].

The numerical approach is based on iterative procedures [11]-[12]. This leads to the burden of computational time to achieve the parameter estimation results. Furthermore, the numerical methods are mostly supported by the gradient-descent procedure tending to converge to local rather than global minima Thus, it is strongly dependent on and influenced by the choice of initialization values of the algorithms which results in a significant deviation between the results of the estimation and experiment. It is realized that both the analytical methods and the numerical methods require a long computation time.

To reduce the computational burden and enhance the efficiency of the existing approaches, stochastic optimization algorithm-based approach is recently introduced to overcome the above-mentioned disadvantages. In a search space, these algorithms do not require predictive information, mainly depend on random initialization and optimization, and especially, can explore multi-dimensions to avoid sticking in locally optimal solutions until the best solution is achieved after the predefined maximum iteration number or accepted error is reached. Amongst the stochastic optimization algorithms,

[1]*School of Engineering, HUTECH University, Ho Chi Minh City, 70000, Vietnam.*
[2]*School of Engineering and Physical Sciences, Heriot-Watt University, Edinburgh, EH14 4AS, United Kingdom.*
**Corresponding author:* Duy C. Huynh; Phone: +84-938-707-507; Email: hc.duy@hutech.edu.vn.

meta-heuristic algorithms are becoming increasingly popular in many applications. These meta-heuristic algorithms are briefly analyzed in the following Table 1.

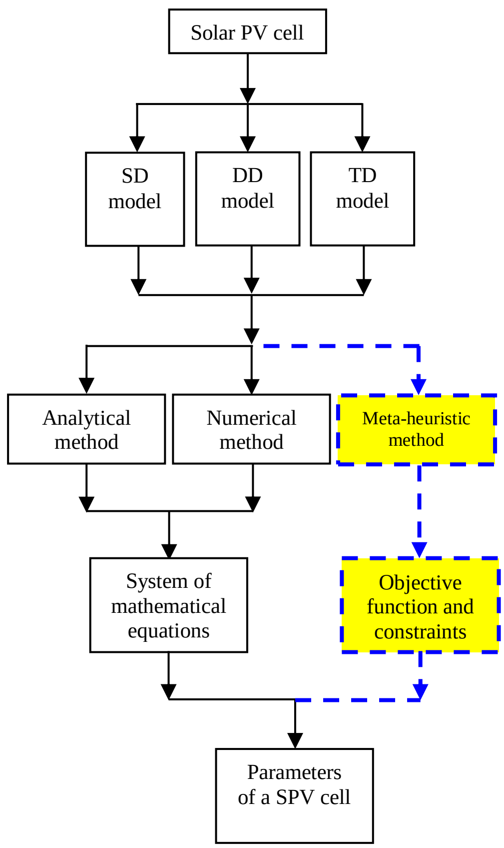

Fig. 1. Parameter estimation proposals for a SPV cell.

It is realized that each algorithm shows its advantages and disadvantages through criteria related to precision and consistency of optimal solutions; performance; and parameters tuning.

Recently, a stochastic fractal search (SFS) algorithm is introduced for many applications [2], [27]. It specially has fewer parameters tuning than COA, ABC, DE, GA, PSO, and EM algorithms [2]. Furthermore, it also easily achieves the globally optimal results with the appropriate number of iterations. In this paper, the SFS algorithm and its variant, called a Chaos SFS algorithm are proposed to solve this problem. The research results demonstrate that the SFS algorithm overcomes the premature convergence and low robustness of other meta-heuristic algorithms. Furthermore, the Chaos SFS algorithm is proposed to direct the local exploitation. The overview and proposals of this problem are described in Fig. 1 where the yellow blocks and blue dashed lines are proposed to improve the accuracy as well as the time to achieve the estimated results.

Table 1 shows that the PSO algorithms are superior to other existing meta-heuristic algorithms. Thus, they should be selected to perform the comparisons with the SFS algorithms. This choice is relevant and competitive.

Table 1. Analysis of meta-heuristic algorithms

Algorithm	Advantage	Disadvantage	Reference
Electromagnetic-like (EM) algorithms	- Effective for continuous optimization problems; - Flexible to global optimization problems.	- Complicated algorithm with 4 procedures including initialization, computation of total force, movement, and local search; - The performance strongly depends on the initial solution; - Poor performance in a local search process.	[13]
Particle swarm optimization (PSO) algorithms	- Fewer parameters tuning; - Easy constraints; - Good for multi-objective optimization.	- Low-quality solution; - Limited memory for updating velocity; - Premature convergence.	[14], [15], [16], [17]
Genetic algorithms (GA)	- Effective with searching optimal solutions; - Good for multi-objective optimization.	- More parameters tuning; - Highly dependent on the parameters tuning; - Difficult to design an objective function; - Computationally expensive.	[12], [18]
Differential evolution (DE) algorithms	- Fewer parameters tuning.	- Significant reliance on the trial vector generating method; - Highly dependent on the selection of the parameter tuning.	[19], [20], [21], [22]
Artificial bee colony (ABC) algorithms	- Simplicity; - Good exploration ability.	- Poor exploitation ability; - Premature convergence.	[3], [23]
Coyote optimization algorithms (COA)	- Fewer parameters tuning; - Diverse mechanisms for balancing exploration and exploitation.	- Computationally expensive; - Poor quality of solutions; - Poor stability in the search process.	[24], [25]

In the remaining, Section 2 is the models of a SPV cell. Section 3 is the application proposal of the SFS algorithms. Section 4 is the application result. Section 5 is the proposal validation.

2. SPV CELL MODELS

2.1. SD model

This SD model is described in Fig. 2 [23].

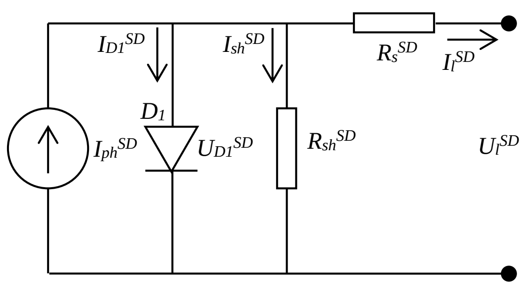

Fig. 2. SD model.

From Fig. 2, the load current in the equivalent circuit is:

$$I_l^{SD} = I_{ph}^{SD} - I_{D1}^{SD} - \frac{U_{D1}^{SD}}{R_{sh}^{SD}} \tag{1}$$

where

$$I_{D1}^{SD} = I_{01}^{SD}\left[\exp\left(\frac{U_{D1}^{SD}}{n_1^{SD}U_t^{SD}}\right) - 1\right] \tag{2}$$

$$U_{D1}^{SD} = U_l^{SD} + R_s^{SD} I_l^{SD} \tag{3}$$

$$U_t^{SD} = \frac{kT}{q} \tag{4}$$

Then, the load current is modified as follows:

$$I_l^{SD} = I_{ph}^{SD} - I_{01}^{SD}\left[\exp\left(\frac{q\left(U_l^{SD} + R_s^{SD} I_l^{SD}\right)}{n_1^{SD}kT}\right) - 1\right] - \frac{U_l^{SD} + R_s^{SD} I_l^{SD}}{R_{sh}^{SD}} \tag{5}$$

where

I_{D1}^{SD} and U_{D1}^{SD}: the current (A) and voltage (V) of D_1 in the SD model;

I_l^{SD} and U_l^{SD}: the load current (A) and voltage (V) in the SD model;

I_{01}^{SD}: the saturation current of D_1 in the SD model (μA);

q: the charge on the electron, $q = 1.602 \times 10^{-19}$ (C);

k: Boltzmann's constant, $k = 1.38 \times 10^{-23}$ (m^2kg/s^2);

T: the absolute temperature of a SPV cell in Kelvin (^{0}K);

R_{sh}^{SD} and R_s^{SD}: the shunt and series resistances in the SD model (Ω);

U_t^{SD}: the panel's thermal voltage in the SD model (V);

I_{ph}^{SD}: the source current in the SD model (A);

n_1^{SD}: the ideality coefficient of D_1 in the SD model.

In this SD model, I_{ph}^{SD}, I_{01}^{SD}, R_s^{SD}, R_{sh}^{SD}, and n_1^{SD} are required to estimate.

2.2. DD model

This DD model is more detailed than the SD model shown in Fig. 3 [3].

Similarly, the load current in the DD model is:

$$I_l^{DD} = I_{ph}^{DD} - I_{01}^{DD}\left[\exp\left(\frac{q\left(U_l^{DD} + R_s^{DD} I_l^{DD}\right)}{n_1^{DD}kT}\right) - 1\right] - I_{02}^{DD}\left[\exp\left(\frac{q\left(U_l^{DD} + R_s^{DD} I_l^{DD}\right)}{n_2^{DD}kT}\right) - 1\right] - \frac{U_l^{DD} + R_s^{DD} I_l^{DD}}{R_{sh}^{DD}} \tag{6}$$

where

I_l^{DD} and U_l^{DD}: the load current (A) and voltage (V) in the DD model;

I_{01}^{DD} and I_{02}^{DD}: the saturation currents of D_1 and D_2 in the DD model (μA);

R_{sh}^{DD} and R_s^{DD}: the shunt and series resistances in the DD model (Ω);

I_{ph}^{DD}: the source current in the DD model (A);

n_1^{DD} and n_2^{DD}: the ideality coefficients of D_1 and D_2 in the DD model.

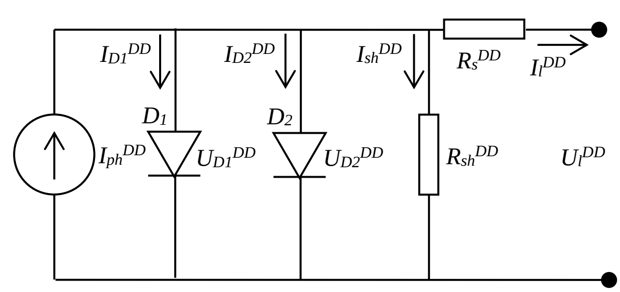

Fig. 3. DD model.

In this DD model, I_{ph}^{DD}, I_{01}^{DD}, I_{02}^{DD}, R_s^{DD}, R_{sh}^{DD}, n_1^{DD}, and n_2^{DD} are required to estimate.

2.3. TD model

This TD model is more detailed than the DD and SD models shown in Fig. 4 [26].

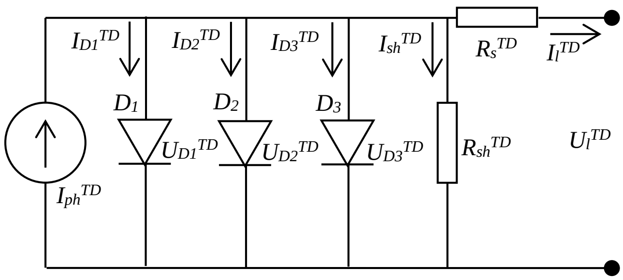

Fig. 4. TD model.

Similarly, the load current in the TD model is given by:

$$\begin{aligned} I_l^{TD} = I_{ph}^{TD} - I_{01}^{TD}\left[\exp\left(\frac{q\left(U_l^{TD}+R_s^{TD}I_l^{TD}\right)}{n_1^{TD}kT}\right)-1\right]- \\ - I_{02}^{TD}\left[\exp\left(\frac{q\left(U_l^{TD}+R_s^{TD}I_l^{TD}\right)}{n_2^{TD}kT}\right)-1\right]- \\ - I_{03}^{TD}\left[\exp\left(\frac{q\left(U_l^{TD}+R_s^{TD}I_l^{TD}\right)}{n_3^{TD}kT}\right)-1\right]- \\ - \frac{U_l^{TD}+R_s^{TD}I_l^{TD}}{R_{sh}^{TD}} \end{aligned} \quad (7)$$

where

I_l^{TD} and U_l^{TD}: the load current (A) and voltage (V) in the TD model;

I_{01}^{TD}, I_{02}^{TD}, and I_{03}^{TD}: the saturation currents of D_1, D_2, and D_3 in the TD model (μA);

R_{sh}^{TD} and R_s^{TD}: the shunt and series resistances in the TD model (Ω);

I_{ph}^{TD}: the source current in the TD model (A);

n_1^{TD}, n_2^{TD}, and n_3^{TD}: the ideality coefficients of D_1, D_2, and D_3 in the TD model.

In this TD model, I_{ph}^{TD}, I_{01}^{TD}, I_{02}^{TD}, I_{03}^{TD}, R_s^{TD}, R_{sh}^{TD}, n_1^{TD}, n_2^{TD}, and n_3^{TD} are required to estimate.

3. PARAMETER ESTIMATION BY SFS ALGORITHMS

The unavailable parameters of the models are estimated by minimizing a root mean square error (RMSE) of the load currents between the experiment and estimation under various scenarios [23].

The RMSE of the load currents is given by:

$$RMSE = \sqrt{\frac{1}{n_{sample}}\sum_{i=1}^{n_{sample}}\left(I_{li}^{est}-I_{li}^{\exp}\right)^2} \quad (8)$$

where

n_{sample}: the sample number;

I_{li}^{exp} and I_{li}^{est}: the i^{th} load currents in the experiment and estimation respectively (A).

The SFS and Chaos SFS algorithms are utilized to solve this problem.

3.1. SFS algorithm

The SFS algorithms are inspired by the growing phenomenon in the nature of random fractals [27]-[28]. Let P be the vector of the estimated parameters including [I_{ph}^{SD}, I_{01}^{SD}, R_s^{SD}, R_{sh}^{SD}, and n_1^{SD}], [I_{ph}^{DD}, I_{01}^{DD}, I_{02}^{DD}, R_s^{DD}, R_{sh}^{DD}, n_1^{DD}, and n_2^{DD}], and [I_{ph}^{TD}, I_{01}^{TD}, I_{02}^{TD}, I_{03}^{TD}, R_s^{TD}, R_{sh}^{TD}, n_1^{TD}, n_2^{TD}, and n_3^{TD}] for the SD, DD, and TD models respectively.

During the diffusion process, the Gaussian walk is chosen to create solutions with a preset maximum diffusion number, n_{md} surrounding each particle for diffusing around its solution as well as implementing the exploitation.

The following is a description of the Gaussian walk.

$$GW = G\left(P_i,\delta\right)+rand\left[0,1\right]\times\left(P_{best}-P_i\right) \quad (9)$$

The Gaussian function is given by:

$$G\left(P_i,\delta\right)=\frac{1}{\delta\sqrt{2\pi}}e^{-\frac{1}{2}\left(\frac{P_{best}-P_i}{\delta}\right)^2} \quad (10)$$

where

G: Gaussian function;

δ: the standard deviation;

P_{best}: the best solution;

P_i: the i^{th} solution, i = 1, 2, 3, ..., n_s;

n_s: the size of swarm.

The standard deviation is as follows:

$$\delta = \left|\frac{\log\left(n_G\right)}{n_G}\times\left(P_{best}-P_i\right)\right| \quad (11)$$

where, n_G is the number of generation.

During the update process, each solution is updated under other solutions. Then, each particle executes the exploration with two statistical procedures.

The first update procedure is:

$$P_i^{'}\left(j\right)=\begin{cases} P_{r1}\left(j\right)-r\times\left[P_{r2}\left(j\right)-P_i\left(j\right)\right] & if\ \ \gamma_i < r \\ P_i\left(j\right) & otherwise \end{cases} \quad (12)$$

where

P'_i: the new solution of P_i;

P_{r1} and P_{r2}: the solutions chosen randomly;

j: the index of each optimization parameter, j = 1, 2, 3, …, d;

d: the number of optimization parameters;

γ_i: the selection probability of a particle, P_i.

$$\gamma_i = 1 - \frac{rank(P_i)}{n_s} \tag{13}$$

where, $rank(P_i)$ is the fitness order of the i^{th} particle in the swarm.

The second update procedure is:

$$P_i^{'}(j) = \begin{cases} P_i(j) - r \times \left[P_{r1}^{'}(j) - P_{best}(j)\right] & if\ r < 0.5 \\ P_i(j) + r \times \left[P_{r1}^{'}(j) - P_{r2}^{'}(j)\right] & otherwise \end{cases} \tag{14}$$

where, P'_{r1} and P'_{r2} are the solutions chosen randomly.

The process of searching and determining the parameters of the models is implemented and ended when the stopping condition is satisfied by the SFS algorithm.

3.2. Chaos SFS algorithm

In the search procedure, the local exploitation should be adaptive around the best solution for enhancing the quality of the final solution. Then, a chaos SFS algorithm is proposed for identifying the best solution as follows [29]:

$$P^{*}(j) = \begin{cases} P_{best}(j) + r \times (2z_k - 1) & if\ \ r < 1 - \dfrac{n_f}{n_{f_{\max}}} \\ P_{best}(j) & otherwise \end{cases} \tag{15}$$

where

P^*: the new solution compared to the worst solution, P_{worst} in the current swarm.

z_k: the chaotic map, $z_k = 4z_{(k-1)}[1-z_{(k-1)}]$ is the logistic map utilized to generate the k^{th} chaotic value;

z_0: the initial chaotic value, $z_0 \in [0,1]$;

n_f and n_{fmax}: the current and maximum numbers of function evaluations.

The flowchart of the SFS and Chaos SFS algorithms is described in Fig. 5. In which, the white blocks and black solid lines represent the SFS algorithm, and the yellow blocks and blue dashed lines represent the Chaos SFS algorithm.

Similarly, the process of searching and determining the parameters of the models is also implemented and ended when the stopping condition is satisfied by the Chaos SFS algorithm.

4. NUMERICAL RESULT

The SFS and Chaos SFS algorithms are applied for estimating the parameters of the SD, DD and TD models. Then, the estimated curves of the SPV cell models are compared to those of the manufacturer's datasheet of the tested cell to validate the proposal [23].

The experiment is implemented with the irradiance, 1000 W/m^2 and the temperature, 33^{0}C. The sample number, n_{sample} is 20. The maximum diffusion number, n_{md} is 1. The numbers of the estimated parameters, d are 5, 7, and 9 in the SD, DD, and TD models respectively.

The swarm size, n_s is 50 and the maximum iteration, $Iter_{max}$ is 1000. These parameters are the same in all algorithms to have a proper comparative condition. The cognitive and social parameters, c_1 and c_2 are 2 in the PSO and Chaos PSO algorithms respectively. The weight factors, w_{PSO} and $w_{ChaosPSO}$ are 0.6 and the logistic map in the PSO and Chaos PSO algorithms respectively [30]-[36].

The solution space of estimated parameters is shown in Table 2.

The estimation results are shown in Tables 3-5 through the estimated currents of each model. These currents are demonstrated in Tables 6-8 by the Chaos SFS algorithm compared to the experimental currents.

Table 2. Solution space of estimated parameters

Parameter	Limit	
	Lower	Upper
I_{ph}^{SD}; I_{ph}^{DD}; and I_{ph}^{TD} (A)	0	1
I_{01}^{SD}; I_{01}^{DD}, I_{02}^{DD}; and I_{01}^{TD}, I_{02}^{TD}, I_{03}^{TD} (μA)	0	1
R_s^{SD}; R_s^{DD}; and R_s^{TD} (Ω)	0	0.5
R_{sh}^{SD}; R_{sh}^{DD}; and R_{sh}^{TD} (Ω)	0	100
n_1^{SD}; n_1^{DD}, n_2^{DD}; and n_1^{TD}, n_2^{TD}, n_3^{TD}	1	2

Table 3. Parameter estimation results in the SD model

Parameter	Algorithm			
	PSO	Chaos PSO	SFS	Chaos SFS
I_{ph}^{SD} (A)	0.73810	0.74852	0.76020	0.76076
I_{01}^{SD} (μA)	0.29170	0.31175	0.30226	0.30910
R_s^{SD} (Ω)	0.03101	0.03202	0.03601	0.03646
R_{sh}^{SD} (Ω)	51.26771	52.35243	52.55642	52.81363
n_1^{SD}	1.27290	1.31851	1.46111	1.47236

Table 4. Parameter estimation results in the DD model

Parameter	Algorithm			
	PSO	Chaos PSO	SFS	Chaos SFS
I_{ph}^{DD} (A)	0.73806	0.74850	0.76010	0.76073
I_{01}^{DD} (μA)	0.29180	0.28160	0.24713	0.24475
I_{02}^{DD} (μA)	0.30158	0.34160	0.36195	0.38038
R_s^{DD} (Ω)	0.03090	0.03211	0.03586	0.03680
R_{sh}^{DD} (Ω)	51.26781	52.35263	53.05625	53.50295
n_1^{DD}	1.27280	1.31830	1.39091	1.45460
n_2^{DD}	1.37624	1.72183	1.78083	1.99615

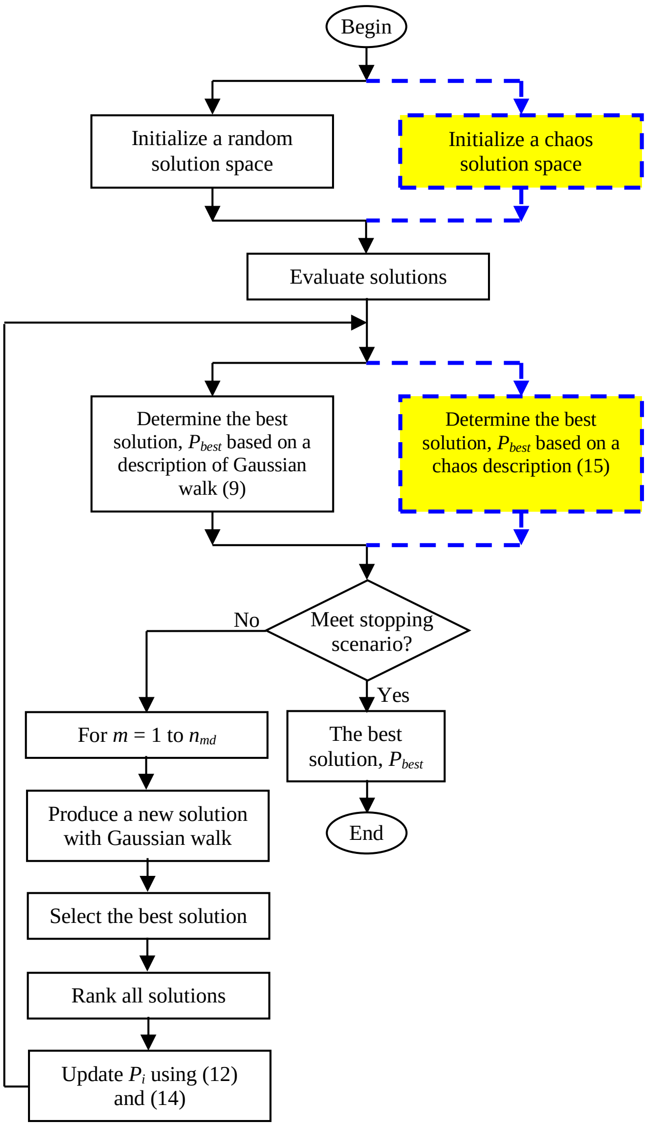

Fig. 5. Flowchart of the SFS and Chaos SFS algorithms.

Table 5. Parameter estimation results in the TD model

Parameter	Algorithm			
	PSO	Chaos PSO	SFS	Chaos SFS
I_{ph}^{TD} (A)	0.72106	0.75115	0.76006	0.76071
I_{01}^{TD} (μA)	0.17531	0.19047	0.20126	0.20947
I_{02}^{TD} (μA)	0.15325	0.16258	0.18614	0.19109
I_{03}^{TD} (μA)	0.19241	0.20761	0.22813	0.23711
R_s^{TD} (Ω)	0.02714	0.02965	0.03261	0.03676
R_{sh}^{TD} (Ω)	50.15314	52.03658	53.48124	53.45398
n_1^{TD}	1.65141	1.82021	1.70615	1.75401
n_2^{TD}	1.18013	1.30865	1.39254	1.43865
n_3^{TD}	2.07627	1.96511	1.92046	1.87025

Table 6. Voltage and current in the SD model by the experiment and estimation using Chaos SFS algorithm

Data	Experiment		Estimation	
	U_l^{SD} (V)	I_l^{SD} (A)	I_l^{SD} (A)	ΔI_l^{SD} (%)
1	0.0057	0.7605	0.76076	0.034
2	0.0646	0.7600	0.75982	0.024
3	0.1185	0.7590	0.75878	0.029
4	0.1678	0.7570	0.75721	0.028
5	0.2132	0.7570	0.75693	0.009
6	0.2545	0.7555	0.75572	0.029
7	0.2924	0.7540	0.75398	0.003
8	0.3269	0.7505	0.75057	0.009
9	0.3585	0.7465	0.74653	0.004
10	0.3873	0.7385	0.73861	0.015
11	0.4137	0.7280	0.72816	0.022
12	0.4373	0.7065	0.70671	0.030
13	0.4590	0.6755	0.67559	0.013
14	0.4784	0.6320	0.63196	0.006
15	0.4960	0.5730	0.57315	0.026
16	0.5119	0.4990	0.49889	0.022
17	0.5265	0.4130	0.41292	0.019
18	0.5398	0.3165	0.31655	0.016
19	0.5521	0.2120	0.21198	0.009
20	0.5633	0.1035	0.10353	0.029

Table 7. Voltage and current in the DD model by the experiment and estimation using Chaos SFS algorithm

Data	Experiment		Estimation	
	U_l^{DD} (V)	I_l^{DD} (A)	I_l^{DD} (A)	ΔI_l^{DD} (%)
1	0.0057	0.7605	0.76073	0.030
2	0.0646	0.7600	0.75964	0.047
3	0.1185	0.7590	0.75881	0.025
4	0.1678	0.7570	0.75718	0.024
5	0.2132	0.7570	0.75686	0.018
6	0.2545	0.7555	0.75569	0.025
7	0.2924	0.7540	0.75383	0.023
8	0.3269	0.7505	0.75048	0.003
9	0.3585	0.7465	0.74621	0.039
10	0.3873	0.7385	0.73882	0.043
11	0.4137	0.7280	0.72816	0.022
12	0.4373	0.7065	0.70681	0.044
13	0.4590	0.6755	0.67525	0.037
14	0.4784	0.6320	0.63171	0.046
15	0.4960	0.5730	0.57296	0.007
16	0.5119	0.4990	0.49915	0.030
17	0.5265	0.4130	0.41306	0.015
18	0.5398	0.3165	0.31641	0.028
19	0.5521	0.2120	0.21193	0.033
20	0.5633	0.1035	0.10346	0.039

Table 8. Voltage and current in the TD model by the experiment and estimation using Chaos SFS algorithm

Data	Experiment		Estimation	
	U_l^{TD} (V)	I_l^{TD} (A)	I_l^{TD} (A)	ΔI_l^{TD} (%)
1	0.0057	0.7605	0.76071	0.028
2	0.0646	0.7600	0.76032	0.042
3	0.1185	0.7590	0.75934	0.045
4	0.1678	0.7570	0.75685	0.020
5	0.2132	0.7570	0.75716	0.021
6	0.2545	0.7555	0.75532	0.024
7	0.2924	0.7540	0.75409	0.012
8	0.3269	0.7505	0.75062	0.016
9	0.3585	0.7465	0.74681	0.042
10	0.3873	0.7385	0.73823	0.037
11	0.4137	0.7280	0.72821	0.029
12	0.4373	0.7065	0.70665	0.021
13	0.4590	0.6755	0.67518	0.047
14	0.4784	0.6320	0.63214	0.022
15	0.4960	0.5730	0.57318	0.031
16	0.5119	0.4990	0.49881	0.038
17	0.5265	0.4130	0.41286	0.034
18	0.5398	0.3165	0.31642	0.025
19	0.5521	0.2120	0.21191	0.042
20	0.5633	0.1035	0.10347	0.029

Table 9 is the error percentages of the load currents between the experiment and Chaos SFS algorithm-based estimation. The maximum, minimum, and average error percentages are shown in Table 10. The more detailed the model, the larger the average error of the load currents between the experiment and estimation is. According to Fig. 6, the average error percentage of the load current in the TD model, 0.0303% is greater than that in the SD and DD models, 0.0188% and 0.0289% respectively. However, the differences in the average error percentages between the TD model; and SD and DD models are not significant, 0.0115% and 0.0014% respectively. All average error percentages are less than 0.0303% and accepted in the parameter estimation application. This means that the results in Tables 3-5 are validated with high accuracy.

Figs. 7-12 respectively demonstrate the *U-I* and *U-P* curves of the models achieved by the experiment and estimation using the Chaos SFS algorithm. These are extremely close together. The achieved parameter estimation results show that the Chaos SFS algorithm has driven the exploitation towards the best estimation result during the search strategy. This is clearly illustrated in Tables 11-13.

Table 9. Error percentage of load current in the models between the experiment and estimation using Chaos SFS algorithm

Data	ΔI_l^{SD} (%)	ΔI_l^{DD} (%)	ΔI_l^{TD} (%)
1	0.034	0.030	0.028
2	0.024	0.047	0.042
3	0.029	0.025	0.045
4	0.028	0.024	0.020
5	0.009	0.018	0.021
6	0.029	0.025	0.011
7	0.003	0.023	0.012
8	0.009	0.003	0.016
9	0.004	0.039	0.042
10	0.015	0.043	0.037
11	0.022	0.022	0.029
12	0.030	0.044	0.021
13	0.013	0.037	0.047
14	0.006	0.046	0.022
15	0.026	0.007	0.014
16	0.022	0.030	0.018
17	0.019	0.015	0.010
18	0.016	0.028	0.025
19	0.009	0.033	0.042
20	0.029	0.039	0.029

Table 10. Maximum, minimum, and average error percentages of the load current in the models between the experiment and estimation using Chaos SFS algorithm

Error percentage (%)	SD model	DD model	TD model
Maximum error percentage (%)	0.034	0.047	0.047
Minimum error percentage (%)	0.003	0.003	0.012
Average error percentage (%)	0.0188	0.0289	0.0303

Figs. 13-15 are the convergence curves of the algorithms.

The Chaos SFS algorithm always has a solution initialization which is better than that in the remaining algorithms. This benefit confirms the efficient role of initializing a solution space based on a chaotic map. Premature convergence always exists in the SFS, Chaos PSO, and PSO algorithms. The shortcoming of premature convergence has been overcome through the procedure of searching and determining the best solution based on a chaotic map. Through the above proposals, the convergence iteration number and the convergence value are significantly improved in the Chaos SFS algorithm. This is a great advantage leading to the accurate and fast parameter estimation results by the Chaos SFS algorithm.

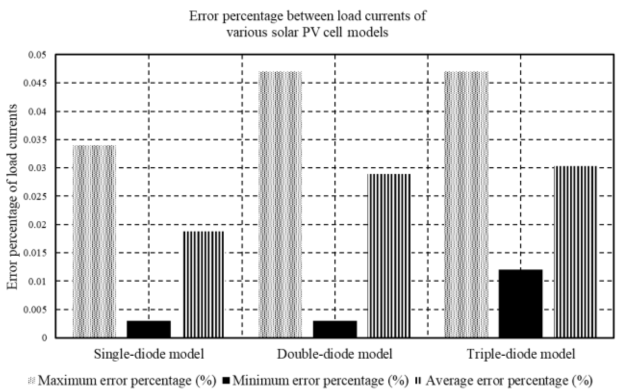

Fig. 6. Error percentages of the load current in the models between the experiment and estimation using Chaos SFS algorithm.

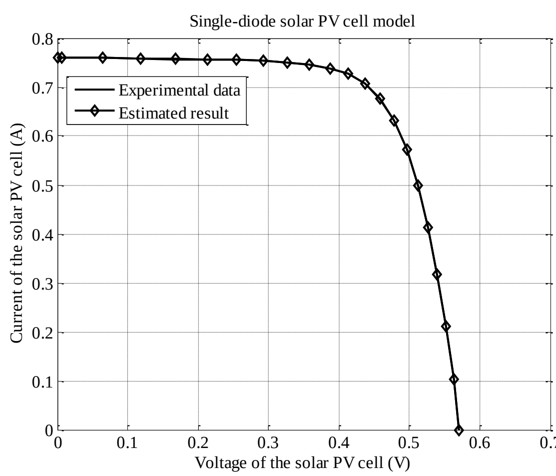

Fig. 7. *U-I* curves in the SD model achieved by the experiment and estimation using Chaos SFS algorithm.

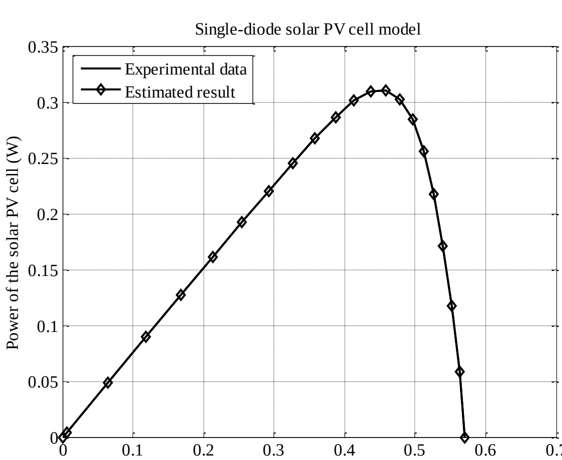

Fig. 8. *U-P* curves in the SD model achieved by the experiment and estimation using Chaos SFS algorithm.

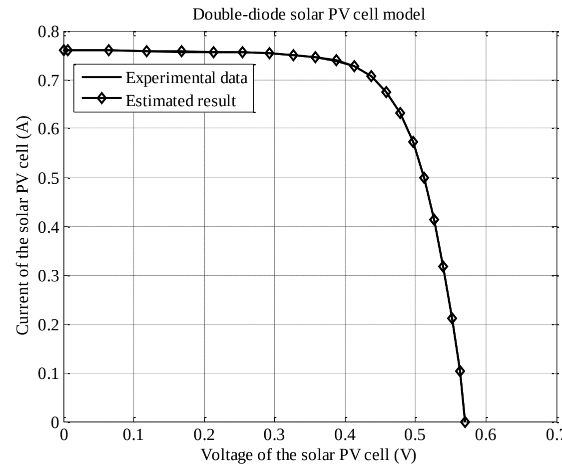

Fig. 9. *U-I* curves in the DD model achieved by the experiment and estimation using Chaos SFS algorithm.

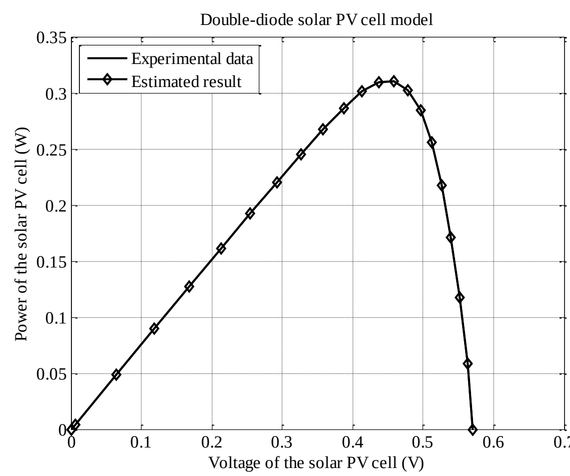

Fig. 10. *U-P* curves in the DD model achieved by the experiment and estimation using Chaos SFS algorithm.

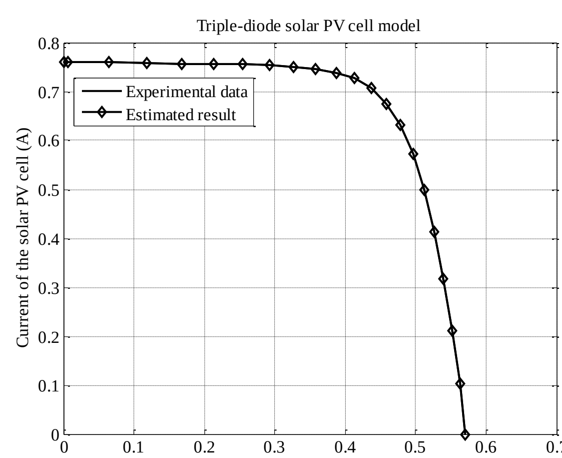

Fig. 11. *U-I* curves in the TD model achieved by the experiment and estimation using Chaos SFS algorithm.

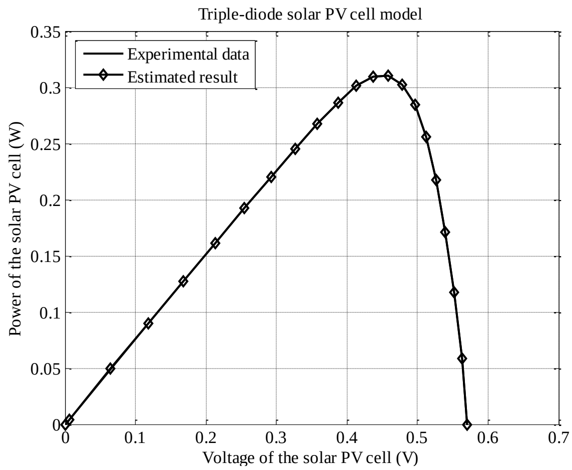

Fig. 12. *U-P* curves in the TD model achieved by the experiment and estimation using Chaos SFS algorithm.

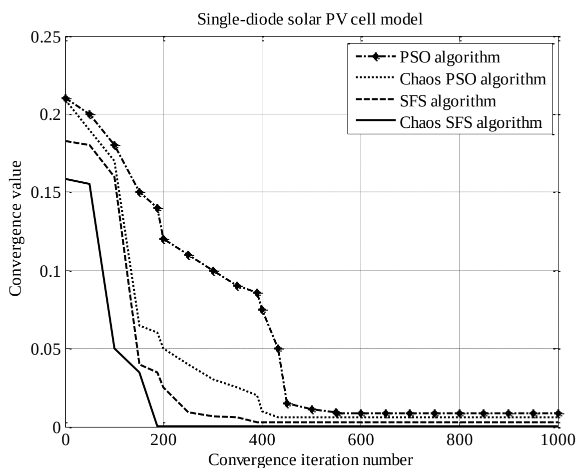

Fig. 13. Convergence curves of the algorithms in the SD model-based parameter estimation.

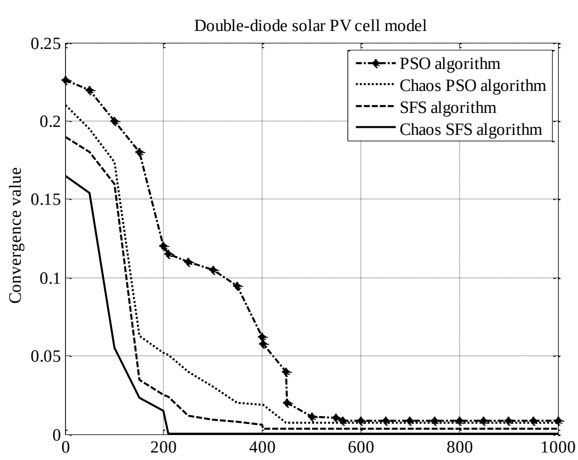

Fig. 14. Convergence curves of the algorithms in the DD model-based parameter estimation.

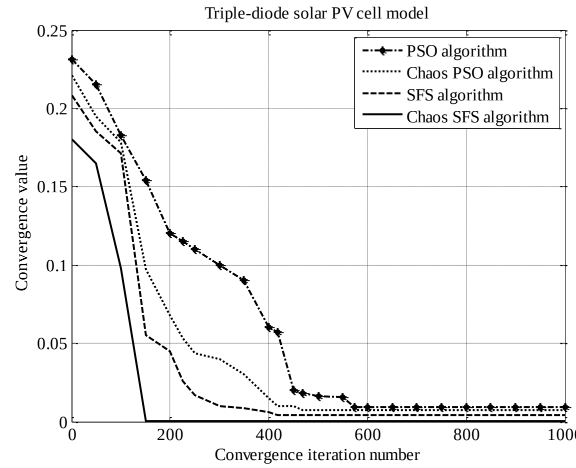

Fig. 15. Convergence curves of the algorithms in the TD model-based parameter estimation.

Table 11. Convergence result of the algorithms in the SD model-based parameter estimation

Algorithm	Convergence value	Convergence iteration
PSO	0.0086	551
Chaos PSO	0.0063	432
SFS	0.0028	389
Chaos SFS	0.000058	187

Table 12. Convergence result of the algorithms in the DD model-based parameter estimation

Algorithm	Convergence value	Convergence iteration
PSO	0.0089	563
Chaos PSO	0.0072	448
SFS	0.0036	401
Chaos SFS	0.000063	209

Table 13. Convergence result of the algorithms in the TD model-based parameter estimation

Algorithm	Convergence value	Convergence iteration
PSO	0.0094	574
Chaos PSO	0.0075	469
SFS	0.0041	418
Chaos SFS	0.000076	226

The convergence value and iteration in the application in the TD model are always greater than those in the SD and DD models, Tables 11-13, because the TD model is more detailed than the SD and DD models. Then, the algorithms must suffer from a computational burden that directly affects the convergence iteration number. However, the effect is not great enough to make the estimation results bad. The convergence values of the Chaos SFS algorithm are still very good enough to ensure the highest accuracy in the parameter estimation results, Tables 3-5. This re-confirms the robustness of the proposed algorithms in this application.

5. CONCLUSION

The SFS and Chaos SFS algorithms are proposed for the parameter estimation of the SD, DD, and TD models. Especially, the Chaos SFS algorithm has overcome the low robustness of the SFS algorithm and the premature convergence of the PSO algorithms.

The achievements confirm the crucial role and effectiveness of chaotic maps in the definition of the solution space and the identification of the optimum solution.

The Chaos SFS algorithm-based estimations are verified for accuracy through comparisons of the error percentage between estimations. The comparisons demonstrate that the error percentages of the Chaos SFS algorithm-based estimations are consistently lower than those using the SFS, Chaos PSO, and PSO algorithms.

REFERENCES

[1] Duy, C. H. and Matthew, W. D. 2016. Development and comparison of an improved incremental conductance algorithm for tracking the MPP of a solar PV panel. IEEE Transactions on Sustainable Energy 7(4): 1421-1429.

[2] Duy, C. H.; Matthew, W. D.; and Corina, B. 2022. Estimation for model parameters and maximum power points of photovoltaic modules using stochastic fractal search algorithm. IEEE Access 10: 104408-104428.

[3] Duy, C. H.; Loc, D. H.; and Matthew, W. D. 2020. Unknown parameter estimation of a detailed solar PV cell model. IEEE Region 10 Conference. Osaka, Japan, 16-19 November: 1-5.

[4] Ma, T.; Yang, H.; and Lu, L. 2014. Solar photovoltaic system modelling and performance prediction. Renewable and Sustainable Energy Reviews 36: 304-315.

[5] Humada, A. M.; Hojabri, M.; Mekhilef, S.; and Hamada, H. M. 2016. Solar cell parameter extraction based on single and double-diode modes: A review. Renewable and Sustainable Energy Reviews 56: 494-509.

[6] Sharadga, H.; Hajimirza, S.; and Cari, E. P. T. 2021. A fast and accurate single-diode model for photovoltaic design. IEEE Journal of Emerging and Selected Topics in Power Electronics 9(3): 3030-3043.

[7] Elkholy, A. and El-Ela, A. A. A. 2019. Optimal parameters estimation and modelling of photovoltaic modules using analytical method. Heliyon 5(7): 1-14.

[8] Ayache, K.; Chandra, A.; Cheriti, A.; and Ouameur, M. A. 2018. AC dynamic parameters extraction of shaded solar cells based on analytical methods and LMLS algorithm. 44th Annual Conference of the IEEE Industrial Electronics Society. Washington, DC, USA, 21-23 October: 1681-1686.

[9] Ćalasan, M.; Abdel-Aleem, S. H. E.; and Zobaa, A. F. 2020. On the root mean square error (RMSE) calculation for parameter estimation of photovoltaic models: A novel exact analytical solution based on Lambert W function. Energy Conversion and Managemen 210: 112716-112734.

[10] Gao, X.; Cui, Y.; Hu, J.; Xu, G.; and Yu, Y. 2016. Lambert W-function based exact representation for double diode model of solar cells: Comparison on fitness and parameter extraction. Energy Conversion and Management 127: 443-460.

[11] Teyabeen, A. A.; Elhatmi, N. B.; Essnid, A. A.; and Jwaid, A. E. 2020. Parameters estimation of solar PV modules based on single-diode model. International Renewable Energy Congress. Hammamet, Tunisia, 29-31 October: 1-6.

[12] Appelbaum, J. and Peled, 2014. A. Parameters extraction of solar cells – A comparative examination of three methods. Solar Energy Materials and Solar Cells 122: 164-173.

[13] Ridha, H. M.; Gomes, C.; and Hizam, H. 2020. Estimation of photovoltaic module model's parameters using an improved electromagnetic-like algorithm. Neural Computing and Applications 32(16): 1-16.

[14] Kiani, A. T.; Nadeem, M. F.; Ahmed, A.; Sajjad, I. A.; Raza, A.; and Khan, I. A. 2020. Chaotic inertia weight particle swarm optimization (CIWPSO): An efficient technique for solar cell parameter estimation. International Conference on Computing, Mathematics and Engineering Technologies. Sukkur, Pakistan, 29-30 January: 1-6.

[15] Yu, K. J.; Ge, S. L.; Qu, B. Y.; and Liang, J. J. 2019. A modified particle swarm optimization for parameters identification of photovoltaic models. IEEE Congress on Evolutionary Computation. Wellington, New Zealand, 10-13 June: 2634-2641.

[16] Duy, C. H. and Matthew, W. D. 2012. Advanced particle swarm optimization algorithms for parameter estimation of a single-phase induction machine," International Journal of Modelling, Identification and Control 15(4): 227-240.

[17] Duy, C. H. 2014. Gauss-PSO parameter identification algorithm for single-phase induction motors. International Journal of Science and Research 3(9): 2360-2364.

[18] Kumar, M. and Rao-K, D. V. S. K. 2019. Modelling and parameter estimation of solar cell using genetic algorithm. International Conference on Intelligent Computing and Control Systems. Madurai, India, 15-17 May: 383-387.

[19] Li, S.; Gong, W.; Yan, X.; Hu, C.; Bai, D.; and Wang, L. 2019. Parameter estimation of photovoltaic models with memetic adaptive differential evolution. Solar Energy 190: 465-474.

[20] Gao, S.; Wang, K.; Tao, S.; Jin, T.; Dai, H.; and Cheng, J. 2021. A state-of-the-art differential evolution algorithm for parameter estimation of solar photovoltaic models. Energy Conversion and Management 230: 243-252.

[21] Wu, Y.; Chen, R.; Li, C.; Zhang, L.; and Cui, Z. 2020. Hybrid symbiotic differential evolution moth-flame optimization algorithm for estimating parameters of photovoltaic models. IEEE Access 8: 156328-156346.

[22] Hao, Q.; Zhou, Z.; Wei, Z.; and Chen, G. 2020. Parameters identification of photovoltaic models using a multi-strategy success-history-based adaptive differential evolution. IEEE Access 8: 35979-35994.

[23] Duy, C. H.; Loc, D. H.; and Matthew, W. D. 2020. Parameter estimation of solar photovoltaic arrays using an artificial bee colony algorithm. Advances in Intelligent Systems and Computing 1284: 281-292.

[24] Diab, A. A. Z.; Sultan, H. M.; Do, T. D.; Kamel, O. M.; and Mossa, M. A. 2020. Coyote optimization algorithm for parameters estimation of various models of solar cells and PV modules. IEEE Access 8: 111102-111140.

[25] Chin, V. J. and Salam, Z. 2019. Coyote optimization algorithm for the parameter extraction of photovoltaic cells. Solar Energy 194: 656-670.

[26] Ramadan, A.; Kamel, S.; Hussein, M. M.; and Hassan, M. H. 2021. A new application of chaos game optimization algorithm for parameters extraction of three diode photovoltaic model. IEEE Access 9: 51582-51594.

[27] Salimi, H. 2015. Stochastic fractal search: a powerful meta-heuristic algorithm. Knowledge-Based Systems 75: 1-18.

[28] Thang, P. V. H. and Tung, T. T. 2017. Economic dispatch in microgrid using stochastic fractal search algorithm. GMSARN International Journal 11(3): 102-105.

[29] Chen, X.; Yue, H.; and Yu, K. 2019. Perturbed stochastic fractal search for solar PV parameter estimation. Energy 189: 1-16.

[30] Duy, C. H. and Matthew. W. D. 2010. Parameter estimation of an induction machine using advanced particle swarm optimization algorithms. IET Electric Power Applications 4(9): 748-760.

[31] Duy, C. H. and Matthew, W. D. 2010. Parameter estimation of an induction machine using a chaos particle swarm optimization algorithm. IET International Conference on Power Electronics, Machines and Drives. Brighton, U.K., 19-21 April: 1-6.

[32] Noopura, S. P.; Sasidharan, S.; Jayan, M. V.; and Tulika, B. 2018. An optimal framework for dynamic energy management in microgrids. GMSARN International Journal 12(2): 76-83.

[33] Anant, O.; Douangtavanh, K.; and Ratchadaporn, O. 2019. Optimal load flow for connection of transmission network in Lao people's democratic republic using particle swarm optimization. GMSARN International Journal 13(4): 183-193.

[34] Witoon, P. and Weerakorn, O. 2016. Multi-objective optimal number of V2G and generation scheduling using improved self-organizing hierarchical particle swarm optimization. GMSARN International Journal 10(2): 47-56.

[35] Duy, C. H. and Nirmal, N. 2015. Chaos PSO algorithm based economic dispatch of hybrid power systems including solar and wind energy sources. IEEE Innovative Smart Grid Technologies - Asia. Bangkok, Thailand, 03-06 November: 1-6.

[36] Duy, C. H. and Loc, D. H. 2016. Improved PSO algorithm based optimal operation in power systems integrating solar and wind energy sources. International Journal of Energy, Information and Communication 7(2): 9-20.